

Two weeks of high glucose intake is enough to induce intestinal mucosal damage and disturb the balance of the gut microbiota of rats

CUNYUN MIN, TINGTING FU, WEI TAN, TINGTING WANG, YU DU and XUHUI HUANG

The Integrated Division of Chinese and Western Medicine, Guangdong Academy of Medical Sciences, Guangdong Provincial People's Hospital, Guangdong Academy of Geriatrics, Guangzhou, Guangdong 510080, P.R. China

Received July 13, 2022; Accepted November 3, 2022

DOI: 10.3892/br.2022.1591

Abstract. High glucose plays a critical role in diabetes. However, the point when high glucose induces diabetes and the organ that triggers the initiation of diabetes remain to be elucidated. The aim of the present study was to clarify the damage induced on different organs of rats, when administered a 2-week infusion of dietary glucose. SD rats (12 weeks old) were randomly divided into normal diet, high glucose infusion (IHG) and oral high glucose (OHG) groups. The levels of fasting blood sugar, tumor necrosis factor (TNF)- α and interleukin (IL)-6 were assessed. Intestine, kidney and liver samples were collected for pathological examination. Feces were collected from the rats for gut microbiota assessment. The results indicated that short-term high glucose induced hyperglycemia that lasted for at least 2 weeks after cessation of high glucose intake. Short-term high glucose also clearly increased the serum levels of IL-6 and TNF- α , led to jejunum mucosa injury and obvious steatosis in hepatocytes, and disturbed the balance of the gut microbiota. OHG led to swelling and necrosis of individual intestinal villi. IHG led to the necrosis and disappearance of cells in the upper layer of the intestinal mucosa. The lesions were confined to the mucosa. A degree of glomerular cell swelling and apoptosis were also observed. Short-term high glucose intake induced lesions in the liver, kidney and intestine, disturbed the balance of the gut microbiota and may consequently induce diabetes complications.

Introduction

The incidence of type 2 diabetes mellitus (T2DM) is rapidly increasing worldwide, which is linked to higher medical costs (1,2). Some progress has been made in treatments for diabetes but their effect is not always sustained and their use may be associated with undesirable side effects, such as hypoglycemia. Insufficient blood glucose control leads to complications and early mortality. The complications of diabetes, such as cardiovascular disease, nephropathy, neuropathy and liver damage, occur shortly after the onset of T2DM (3). Clinical experiments have confirmed the 'legacy effect' or 'metabolic memory' of prior glycemic control. The long-term cardiovascular benefits of good glycemic control early in the course of diabetes is receiving increasing attention (4,5). Increasing evidence suggests that numerous patients with T2DM can follow a non-albuminuric pathway to renal function loss, even after accounting for the use of renoprotective agents (6,7). It is important to clarify the association between high glucose intake and the formation of diabetes. Hyperglycemia is critical in the genesis of diabetic complications. Poor glycemic control is an independent predictor of the development and progression of diabetic complications. The tight control of glucose concentration is determined by glucose absorption from the intestine, glucose production by the liver and glucose uptake from the plasma (8). Patients with T2DM are prone to developing nonalcoholic fatty liver disease (NAFLD), and NAFLD itself is associated with a risk of T2DM. It has been revealed that a number of patients with chronic liver disease have an abnormal glucose metabolism, which ultimately leads to impaired glucose tolerance and the development of diabetes. The pathogenesis of impaired glucose metabolism during chronic liver disease has yet to be fully elucidated. The potential of targeting the liver to normalize blood glucose levels has not been fully exploited (9-11). The molecular mechanisms controlling hepatic gluconeogenesis and glycogen storage are not very clear, deeming further clinical and experimental studies necessary. The time it takes for high glucose to induce liver lesions needs to be determined.

The gut microbiota is a large and complex microbial ecosystem that maintains the homeostasis of the body and environment. The microbiota consumes carbohydrates that are

Correspondence to: Dr Cunyun Min, The Integrated Division of Chinese and Western Medicine, Guangdong Academy of Medical Sciences, Guangdong Provincial People's Hospital, Guangdong Academy of Geriatrics, 106 Zhongshan 2nd Road, Guangzhou, Guangdong 510080, P.R. China
E-mail: mcy1288@163.com; mincunyun@gdph.org.cn

Key words: high glucose infusion, oral high glucose, liver, intestinal mucosa, gut microbiota, kidney

not easily digested by the body. The human gut microbiome is a promising target for managing T2DM. Short-chain fatty acids (SCFAs) are produced through the fermentation of dietary fiber by the gut microbiota and are beneficial to the health of the body. Insufficient production of SCFAs is associated with T2DM (12,13). This indicates that intestinal mucosa and gut microbiota play an important role in glycemic control. However, the changes that occur in the intestinal mucosa and gut microbiota following short-term high glucose intake are not clear.

Sugar consumption is regarded as a major risk for the development of obesity. Diets enriched in sugars including the intake of sugar-sweetened beverages have been consistently linked to the increased risk of obesity, T2DM, and cardiovascular disease. Dietary glucose has been revealed to increase serum glucose and insulin concentrations in the postprandial state. Studies in experimental animals and in humans have demonstrated that chronic elevation in the plasma glucose concentration impairs insulin action. Chronic hyperglycemia causes insulin resistance, but the short-term glucotoxicity and the underlying mechanisms are unclear (14,15).

High glucose plays a critical role in the formation and progression of diabetes. However, the mechanism through which it induces diabetes and the organ that triggers diabetes remain unclear. The scope of most studies is restricted to studying the effects of oral high glucose (OHG) or high glucose infusion (IHG) on only one or two organs. Therefore, the aim of the present study was to evaluate the different effects of short-term OHG or IHG on different organs concurrently. Rats were fed or infused with liquid high glucose, and the effects on the liver, pancreas, kidneys and intestine, as well as the development of gut microbial dysbiosis, were analyzed.

Materials and methods

Experimental animals. The present study was performed using 30 male specific pathogen-free Sprague-Dawley rats aged 12 weeks and weighing $\sim 200 \pm 20$ g. The rats were purchased from the Experimental Animal Center of Guangdong Province [approval no. SCXK (Yue)-2013-0002]. All rats were raised under light-controlled conditions (12-h light/dark cycle) in a temperature- ($23 \pm 2^\circ\text{C}$) and humidity (40%)-controlled room with food and water freely available.

All animal experiments were conducted in accordance with the guidelines of the Ethics Committee of the Guangdong Provincial People's Hospital (Guangzhou, China) and approved (approval no. KY-D-2019-082-01) by the Institutional Animal Care and Use Committee of Guangdong Provincial People's Hospital.

Experimental design. Following adaptive feeding, all rats were randomly divided into three groups: The normal diet (ND; $n=10$), the OHG ($n=10$) and the IHG ($n=10$) groups. OHG group rats were fed with 50% high glucose at a dose of 2.5 g/kg/day for 2 weeks. The IHG group rats were treated with 50% high glucose via tail vein injection at a dose of 2 g/kg/day for 2 weeks. The ND group received an equivalent amount of saline orally for the same period. During the experiment, all rats received the same standard chow. Fasting blood sugar (FBS) levels were measured in all animals weekly using

a glucometer (Abbott Diabetes Care). Finally, all rats were sacrificed by cervical dislocation following anesthesia with an intraperitoneal injection of sodium pentobarbital (45 mg/kg; MilliporeSigma) to reduce pain. The following samples were collected from the rats: Feces were collected individually for at least 3 days for each animal. Blood samples were collected via the abdominal aorta (4 ml) for biochemical assays after anesthesia with an intraperitoneal injection of sodium pentobarbital. Intestine and liver samples were also collected.

Weight of rats. The weight of the rats was measured at different time-points (days 1, 8, 16, 24 and 32), to determine the effect of high glucose on the ND, OHG and IHG groups.

Changes in blood glucose levels. In order to compare the effects of IHG and OHG on blood glucose levels, FBS levels were measured on days 0 (prior to glucose intake), 18, 24 and 32.

Detection of cytokines and chemokines. ELISA kits were used to measure the serum levels of pro-inflammatory cytokines interleukin (IL)-6 (cat. no. ERA31RB), tumor necrosis factor (TNF)- α (cat. no. BMS622), blood insulin (BI) (cat. no. ERINS; all from Invitrogen; Thermo Fisher Scientific, Inc.) and 24-h microalbuminuria (cat. no. BJ003256; Shanghai Bangjing Industrial Co., Ltd.) according to the manufacturer's instructions. The blood glutamic pyruvic transaminase (ALT; cat. no. BC1555) and glutamic oxalic transaminase (AST; cat. no. BC1565; both from Beijing Solarbio Science & Technology Co., Ltd.) levels were determined using standard enzymatic kits.

Histopathological examinations. The jejunum was removed, divided longitudinally, and washed. The intestine, liver, kidney and pancreatic sections (4 mm) were fixed in 10% formalin for 2 h at 25°C , embedded in paraffin and stained with hematoxylin and eosin for 3 min at 25°C . Oil Red O staining for 5 min at 25°C was performed on frozen sections (2 mm) fixed in 4% paraformaldehyde for 6 h at 25°C and sucrose-protected. For the comparison of histological differences, three sections were blindly selected per sample from each rat and quantified using ImageJ software (version 1.6.0; National Institutes of Health). Kidney sections (2 mm) were fixed in 2.5% neutral glutaraldehyde (cat. no. A17876; Alfa Aesar; Thermo Fisher Scientific, Inc.) for 3 h at 4°C , stained with 2% uranyl acetate (cat. no. 22400; Electron Microscopy Sciences) for 30 min at 25°C , for assessment using transmission electron microscopy (JEM-1400 PLUS; Japan Electron Optics Laboratory Co., Ltd.).

Western blotting. In order to detect changes in renal cells, the levels of gasdermin D (GSDMD), NLR family pyrin domain containing 3 (NLRP3) and caspase-1 protein were assessed to determine whether apoptosis occurred in renal cells. Western blotting was performed on total protein extracts from rat kidneys ($n=3$ per group). Lysis buffer (cat. no. ab270054, Abcam) was used for protein extraction. BCA protein assay was used for protein determination. A total of 50 μg protein/lane was separated on 13.5% SDS-PAGE gel and transferred onto a PVDF membrane for 1 h at 100V. Subsequently, 10X Blocking Buffer (cat. no. ab126587; Abcam) was used to block the membrane to prevent non-specific background binding of the

primary and secondary antibodies to the membrane at 25°C for 1 h. The blots were immunoprobed with anti-GSMD (dilution, 1:500; cat. no. 219800), anti-caspase-1 (dilution, 1:500; cat. no. ab138483), and mouse anti-NLRP3 (dilution, 1:1,000; cat. no. ab263899; all from Abcam) and rabbit anti-GAPDH (dilution, 1:1,000; cat. no. 25778; Santa Cruz Biotechnology, Inc.) antibodies, incubated at 25°C for 1 h. Pierce ECL Western Blotting Substrate (cat. no. 32106; Thermo Fisher Scientific, Inc.) was used for the detection of the anti-rabbit HRP-conjugated secondary antibody (dilution, 1:500; cat. no. AC2114; Azure Biosystems) at 25°C for 2 h. Films were scanned using the RICOH scanner (600 dpi and grey scale) and analyzed with ImageJ software (version 1.6.0; National Institutes of Health).

Gut microbiota analysis.

DNA extraction and PCR amplification. Microbial DNA was extracted from the feces of rats using the HiPure Soil DNA Kits (cat. no. D3143-03; Shanghai Maige Biotechnology Co., Ltd.), according to the manufacturer's instructions. As the most popular method used for 16S assessment, the 16S rDNA V4 region of the ribosomal RNA gene was amplified using PCR (95°C for 2 min, followed by 27 cycles at 98°C for 10 sec, 62°C for 30 sec and 68°C for 30 sec, followed by a final extension at 68°C for 10 min). The following primers were used: 341F CCTACGGGAGGCAGCAG, 806R GGACTACHVGGGTWTCTAAT, 515F GTGYCAGCMGCCGCGGTAA, 806R GGACTACHVGGGTWTCTAAT. Arch519F, CAGCTGCCGCGGTAA and Arch915R, GTGCTCCCCCGCAATTCCT were used as a supplement, where the barcode is an 8-base sequence unique to each sample. PCR reactions were performed in triplicate in 50 µl mixture containing 5 µl of 10X KOD Buffer, 5 µl of 2.5 mM dNTPs, 1.5 µl of each primer (5 µM), 1 µl KOD Polymerase, and 100 ng template DNA. Amplicons were extracted from 2% agarose gels and purified using the AxyPrep DNA Gel Extraction Kit (Corning, Inc.), according to the manufacturer's instructions, and quantified using ABI StepOnePlus Real-Time PCR System (Thermo Fisher Scientific, Inc.). Purified amplicons were pooled in equimolar and paired-end sequenced (2x250) on an Illumina platform according to the manufacturer's instructions. The raw reads were deposited into the NCBI Sequence Read Archive database (accession no. PRJNA884142; ID:884142).

Bioinformatics analysis. Raw data were further filtered using FASTP (<https://github.com/OpenGene/fastp>) as follows: i) Removing reads containing >10% of unknown nucleotides (N); ii) Removing reads containing <80% of bases with quality (Q-value) >20. Paired end clean reads were merged as raw tags using FLASH (version 1.2.11; <http://ccb.jhu.edu/software/FLASH/index.shtml>) with a minimum overlap of 10 bp and mismatch error rates of 2%. Noisy sequences of raw tags were filtered using QIIME (version 1.9.1; <http://www.wernerlab.org/software/macqiime>) under specific filtering conditions to obtain the high-quality clean tags. Clean tags were searched against the reference database (http://drive5.com/uchime/uchime_download.html) to perform reference-based chimera checking using UCHIME algorithm (http://www.drive5.com/usearch/manual/uchime_algo.html). All chimeric tags were removed

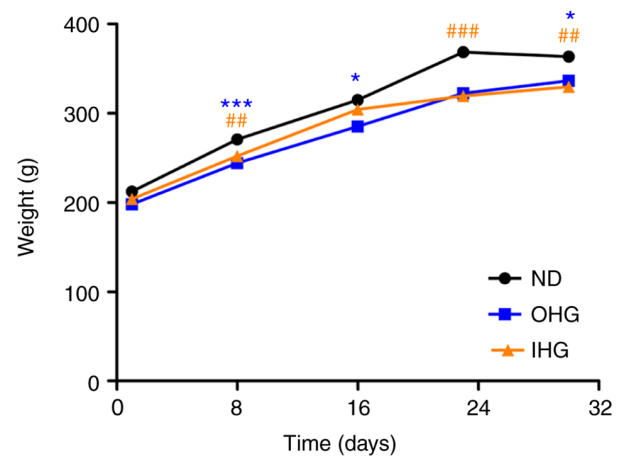


Figure 1. Weight change of rats. The weights of rats in the OHG and IHG groups were lower than those in the ND group. Data are presented as the mean \pm SD; n=10. *P<0.05 and ***P<0.01, the OHG group vs. the ND group; **P<0.01 and ***P<0.01, the IHG group vs. the ND group. No obvious differences were identified between OHG intake and IHG. OHG, oral high glucose; IHG, high glucose infusion; ND, normal diet.

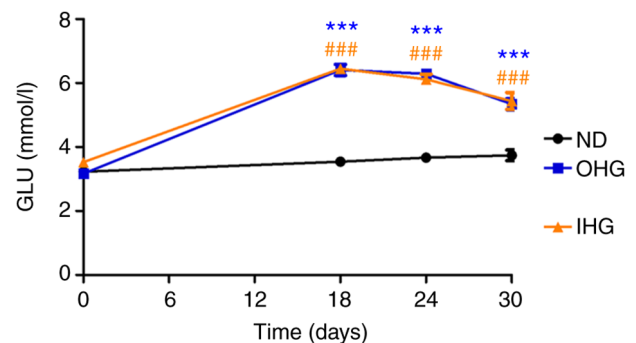


Figure 2. Change of blood glucose. The blood glucose levels of rats in the OHG and IHG groups were significantly higher than those in rats of the ND group until 14 days after ceasing glucose intake. No differences were identified between OHG intake and IHG. ***P<0.01, the OHG group vs. the ND group; ***P<0.01, the IHG group vs. the ND group. OHG, oral high glucose intake; IHG, high glucose infusion; ND, normal diet.

and the effective tags that were finally obtained were used for further analysis. The effective tags were clustered into operational taxonomic units (OTUs) of $\geq 97\%$ similarity using UPARSE (<https://ext.dcloud.net.cn/>). The tag sequence with highest abundance was selected as a representative sequence within each cluster. Venn analysis between groups was performed in the R project (version 3.4.1; <http://ruanfujia.com/vendor/3191173>) to identify unique and common OTUs. The representative sequences were classified into organisms using RDP classifier (version 2.2), a naive Bayesian model, on the SILVA database (<https://www.arb-silva.de/>), with the confidence threshold values ranging from 0.8 to 1. The abundance statistics of each taxonomy were visualized using Krona (version 2.6; <https://github.com/marbl/Krona/wiki>). Biomarker features in each group were screened by Metastats (version 20090414; <http://www.mothur.org/wiki/Metastats>) and LEfSe software (version 1.0; <http://cloud.magiene.com>). Chao1, Simpson and all other alpha diversity indices were calculated in QIIME. OTU rarefaction curve and rank

abundance curves were plotted in QIIME. Alpha index comparison between groups was calculated via Welch's t-test and Wilcoxon rank test in the R project. Alpha index comparison among groups was computed by Tukey's HSD test and Kruskal-Wallis H test in the R project. Weighted and unweighted unifracs distance matrices were generated by QIIME. Multivariate statistical techniques, including principal component analysis, principal coordinates analysis and non-metric multi-dimensional scaling of unweighted nifrac distances were calculated and plotted in the R project. Statistical analysis of Welch's t-test, Wilcoxon rank test, Tukey's HSD test, Kruskal-Wallis H test, Adonis (also called Permanova) and Anosim test was calculated using the R project. The Kyoto Encyclopedia of Genes and Genomes (KEGG) pathway analysis of the OTUs was conducted using Tax4Fun (version 1.0; <http://tax4fun.gobics.de/>).

Statistical analysis. All the experiments were independently performed more than three times. The data are expressed as the mean \pm standard deviation. Statistical analysis was performed using SPSS 21.0 (IBM, Corp.). Statistical differences were determined using a one-way ANOVA with Tukey's post hoc test. $P < 0.05$ was considered to indicate a statistically significant difference.

Results

Weight of rats. To compare the effect of a IHG and OHG on the weight of rats, their weight was measured on days 1, 8, 16, 24 and 32. The weight of the rats in the OHG and IHG groups was lower than that in the ND group (Fig. 1). Loss of appetite caused by high blood glucose and damage of intestinal mucosa may be the reasons for the recorded weight loss. However, the exact reasons warrant further study.

Biochemical observations. In order to compare the influence of IHG and OHG on blood glucose levels, FBS levels were measured at days 0 (prior to glucose intake), 18 24 and 30. Both OHG and IHG significantly increased blood glucose levels. Blood glucose was slowly decreased 7 days after ceasing glucose intake in both groups. The blood glucose levels in both groups of rats were higher than that in rats with a ND until 14 days after ceasing high glucose intake. There was no difference between the OHG and IHG groups (Fig. 2).

At the end of high glucose intake, the serum levels of inflammatory cytokines IL-6 and TNF- α were measured to evaluate the level of inflammation in rats. The serum levels of IL-6 and TNF- α were markedly increased in both the OHG and IHG groups. However, the increase was slightly more in the IHG group than in the OHG group (Table I).

The blood insulin, blood ALT and AST levels, as well as urinary protein content, were assessed to detect the function of the pancreas, liver and kidneys. No obvious differences were identified among the three groups (Table II). In addition, no urinary protein was detected (data not shown).

Histopathological observations. Hepatic fat accumulation was investigated 14 days after ceasing high glucose intake. Both OHG and IHG induced obvious steatosis in the livers of rats. A

Table I. Expression levels of cytokines, IL-6 and TNF- α , in the blood.

Groups (n=10)	IL-6 (pg/ml)	TNF- α (pg/ml)
OHG	122 \pm 11.16 ^a	295.28 \pm 36.95 ^a
IHG	127.8 \pm 16.42 ^{a,b}	300.28 \pm 30.1 ^{a,b}
ND	89.49 \pm 18.24	245.85 \pm 34.46

^a $P < 0.01$ compared with the ND group; and ^b $P < 0.05$ compared with the OHG group. Compared with the ND group, the blood IL-6 and TNF- α levels of rats significantly increased after 2 weeks of OHG and IHG. IL, interleukin; TNF, tumor necrosis factor; OHG, oral high glucose; IHG, high glucose infusion, ND, normal diet.

Table II. Assessment of BI, ALT and AST.

Groups (n=10)	BI (U/l)	ALT (U/l)	AST (U/l)
OHG	22.3 \pm 5.16 ^a	45.28 \pm 3.95 ^a	123.45 \pm 5.42 ^a
IHG	22.8 \pm 4.42 ^{a,b}	46.28 \pm 4.1 ^{a,b}	124.33 \pm 5.26 ^{a,b}
ND	21.9 \pm 4.24	45.85 \pm 4.46	123.98 \pm 6.12

^a $P > 0.05$ compared with the ND group; and ^b $P > 0.05$ compared with the OHG group. There were no significant differences between three groups. BI, blood insulin; ALT, glutamic pyruvic transaminase; AST, glutamic oxalic transaminase; OHG, oral high glucose; IHG, high glucose infusion, ND, normal diet.

large number of hepatocytes were injured. A large amount of white fat could be observed in the sections of the OHG and the IHG groups, which was due to liver cell lipolysis. No differences between the OHG and IHG groups were identified (Fig. 3).

Jejunum mucosae were collected from rats for pathological assessment. Both OHG and IHG induced jejunum mucosa injury. In the jejunum tissue, there was no obvious lesion in the intestinal mucosa of the ND group. In the OHG group, a small amount of intestinal mucosal villi had atrophied, villi epithelial cells were damaged, individual villi had swelled and died, and epidermal epithelial cells had disappeared. In the IHG group, intestinal mucosal villi had atrophied. In addition, a large number of cells in the upper intestinal mucosa were necrotic, and the normal structure of the villi had disappeared, but the lesions were limited to the mucosal layer. The results revealed that high glucose or IHG for 2 weeks causes jejunum lesions (Fig. 4).

Following observation under an optical microscope, no obvious pathological lesions were identified in the kidney and pancreatic tissues of the rats (Fig. 5). Following transmission electron microscopy, however, a degree of glomerular cell swelling was identified, the internal structure of mitochondria was found to be empty and mitochondria were disintegrated (Fig. 6).

Glomerular cell apoptosis. Since the kidney is one of the targets of glycotoxins, the kidney was examined for pathological lesions; no obvious lesions were identified (Fig. 5). One of the objectives of the present study was to clarify whether high glucose induces renal cell damage. Apoptosis is a common type of cell death (16). GSMD, caspase-1 and NLRP3 were

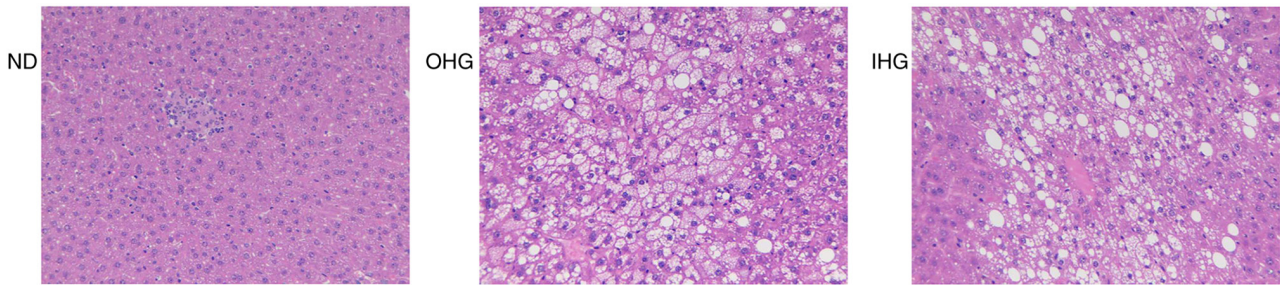


Figure 3. Damage of glucose in the liver. The normal diet group, oral high-glucose intake group and high glucose infusion groups are presented. Both oral high glucose and high glucose infusion led to steatosis in the livers of rats. Magnification, x200.

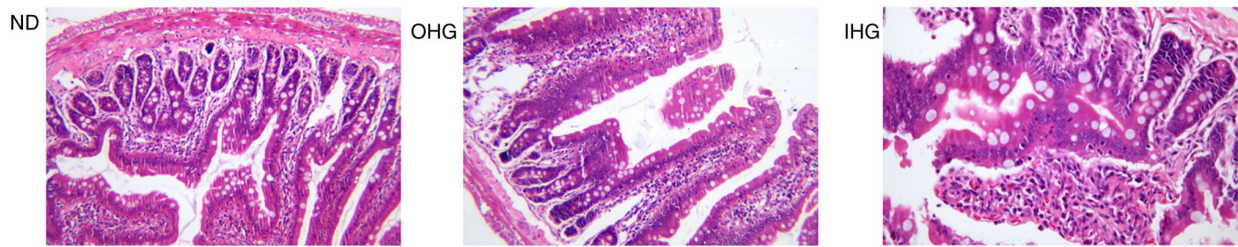
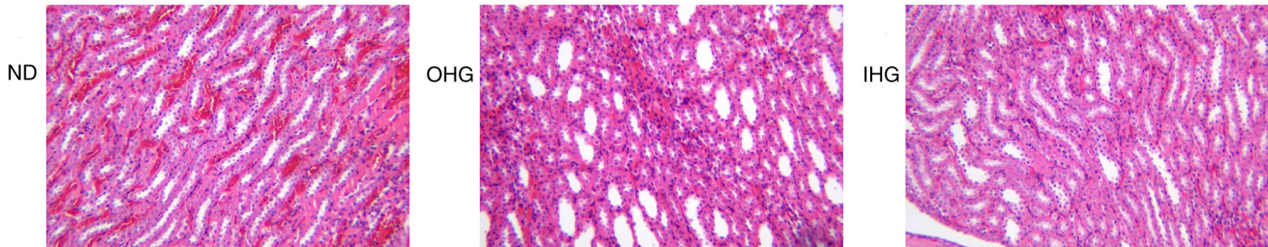


Figure 4. Damage of high glucose to intestinal mucosa. Oral high glucose led to swelling and necrosis of individual intestinal villi and some epithelial cells disappeared. High glucose infusion led to necrosis and the disappearance of cells in the upper layer of the intestinal mucosa. The lesions were confined to the mucosa. Magnification, x200.

Kidney



Pancreas

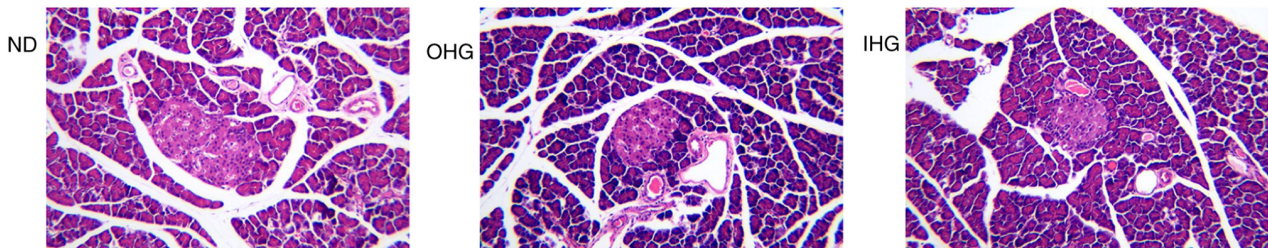


Figure 5. Pathological changes of the kidneys and pancreas. There were no obvious pathological changes in the kidneys and pancreas of rats. Compared to the ND group there were no obvious pathological changes in the kidneys and pancreas of the OHG and IHG groups. Magnification, x200.

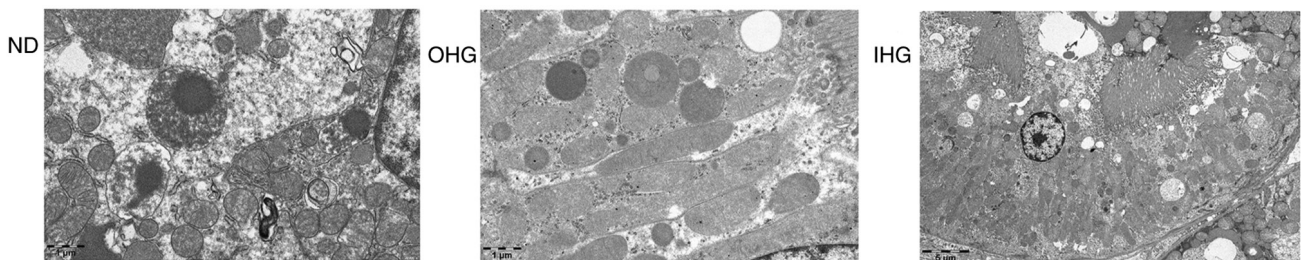


Figure 6. Results of transmission electron microscopy. High glucose induced glomerular cell swelling. The internal structure of mitochondria became empty and mitochondria disintegrated. Magnification, x5,000.

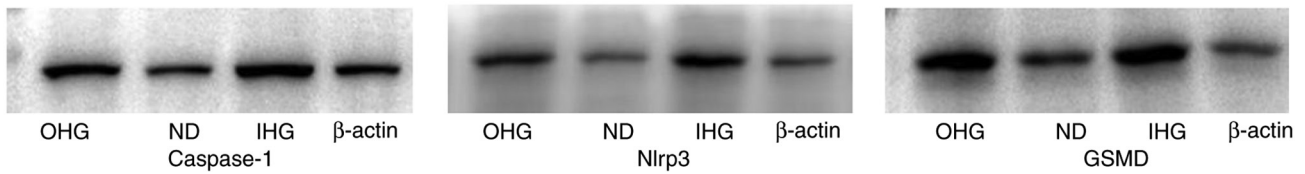


Figure 7. Renal apoptosis. The expression levels of caspase-1, NLRP3 and GSMD in the kidneys of rats was increased. From left to right: the OHG group, the ND group, the IHG group and β -actin. NLRP3, NLR family pyrin domain containing 3; GSMD, gasdermin D; OHG, oral high glucose; ND, normal diet; IHG, high glucose infusion.

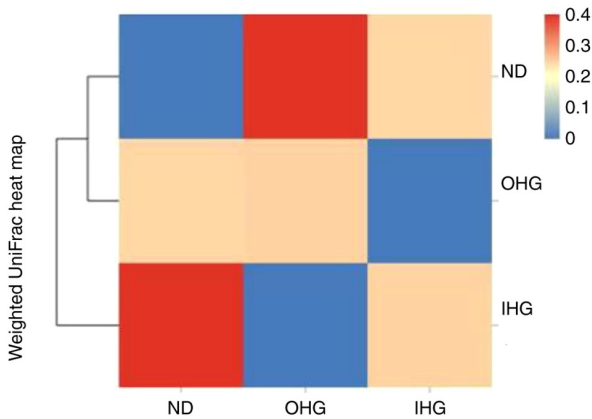


Figure 8. Weighted UniFrac heat map. Gut microbiota was altered after high glucose intake.

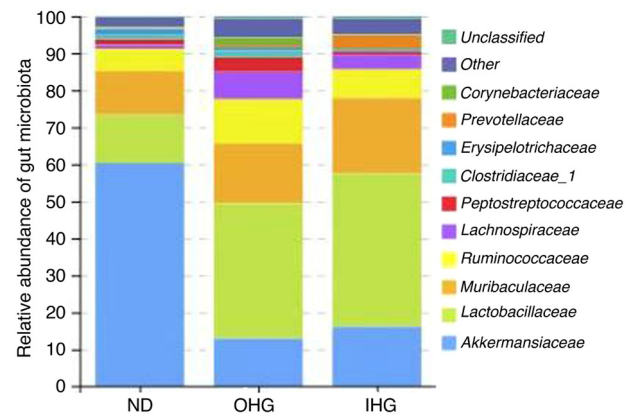


Figure 9. Relative abundance of gut microbiota.

assessed to confirm the apoptosis of renal cells. The expression levels of GSMD, caspase-1 and NLRP3 were increased in the kidney (Fig. 7). This indicated that glomerular cells were damaged to a certain extent.

Changes in the gut microbiota. To elucidate the mechanism of the effect of high glucose, the impact of high glucose on the gut microbiota was investigated in SD rats. 16S rDNA sequencing was used to assess changes in the fecal microbiota of OHG and IHG rats. The dominant floras in the rat intestines were *Akkermansiaceae*, *Lactobacillaceae*, *Muribaculaceae*, *Ruminococcaceae*, *Peptostreptococcaceae*, *Clostridiaceae_1*; these accounted for 60% of the gut microbiota in SD rats. Rats in the two groups lost gut microbial diversity. It was characterized by a lower proportion of *Akkermansiaceae* and a markedly increased proportion of *Lactobacillaceae*, *Muribaculaceae*, *Ruminococcaceae*, *Peptostreptococcaceae*.

Compared with the ND group, the abundance of *Akkermansiaceae* was decreased in the OHG group, while that of *Lactobacillaceae*, *Muribaculaceae*, *Ruminococcaceae* and *Clostridiaceae_1* was increased in the OHG group. The abundance of *Akkermansiaceae* and *Clostridiaceae_1* was decreased in the IHG group. The abundance of *Lactobacillaceae* and *Muribaculaceae* was increased in the IHG group (Figs. 8-10).

Discussion

Sugar consumption is regarded as a major risk for the development of obesity and diabetes. Prediabetes or intermediate hyperglycemia is a high-risk state for developing T2DM (17,18).

The effects of OHG and IHG on blood glucose were compared, and it was revealed that both markedly increased blood glucose. In addition, both also led to persistent hyperglycemia that lasted two weeks. Notably, it was demonstrated that both OHG and IHG caused weight loss in rats. These results confirmed that sugar is a critical cause of diabetes.

Inflammation is divided into two complementary subsystems: The innate immune system and the highly adaptive immune system. An increasing number of studies has indicated that diabetes is a type of inflammation (19,20). It is now accepted that obesity-associated chronic low-grade systemic inflammation is a major underlying factor for the development of several metabolic diseases (21). The present results indicated that only 2 weeks of OHG or IHG induced inflammation in rats.

Clinical and pathophysiological studies have shown that T2DM is a condition mainly caused by excess fat accumulation in the liver and pancreas. Excess fat worsens hepatic responsiveness to insulin, leading to increased glucose production. The removal of excess fat from the liver through substantial weight loss can normalize hepatic insulin responsiveness (22,23). Negative energy balance in T2DM causes a marked decrease in liver fat content, which results in the normalization of hepatic insulin sensitivity within 7 days. As the period of negative energy balance extends, liver fat levels decrease to the normal range and the rate of export of triacylglycerols from the liver also decreases (24).

The primary care-based Diabetes Remission Clinical Trial revealed that 46% of patients with T2DM could achieve remission, which was mediated by weight loss, at 12 months, and 36% at 24 months (25,26). Glucotoxicity and lipotoxicity are key factors of T2DM, but their molecular nature during

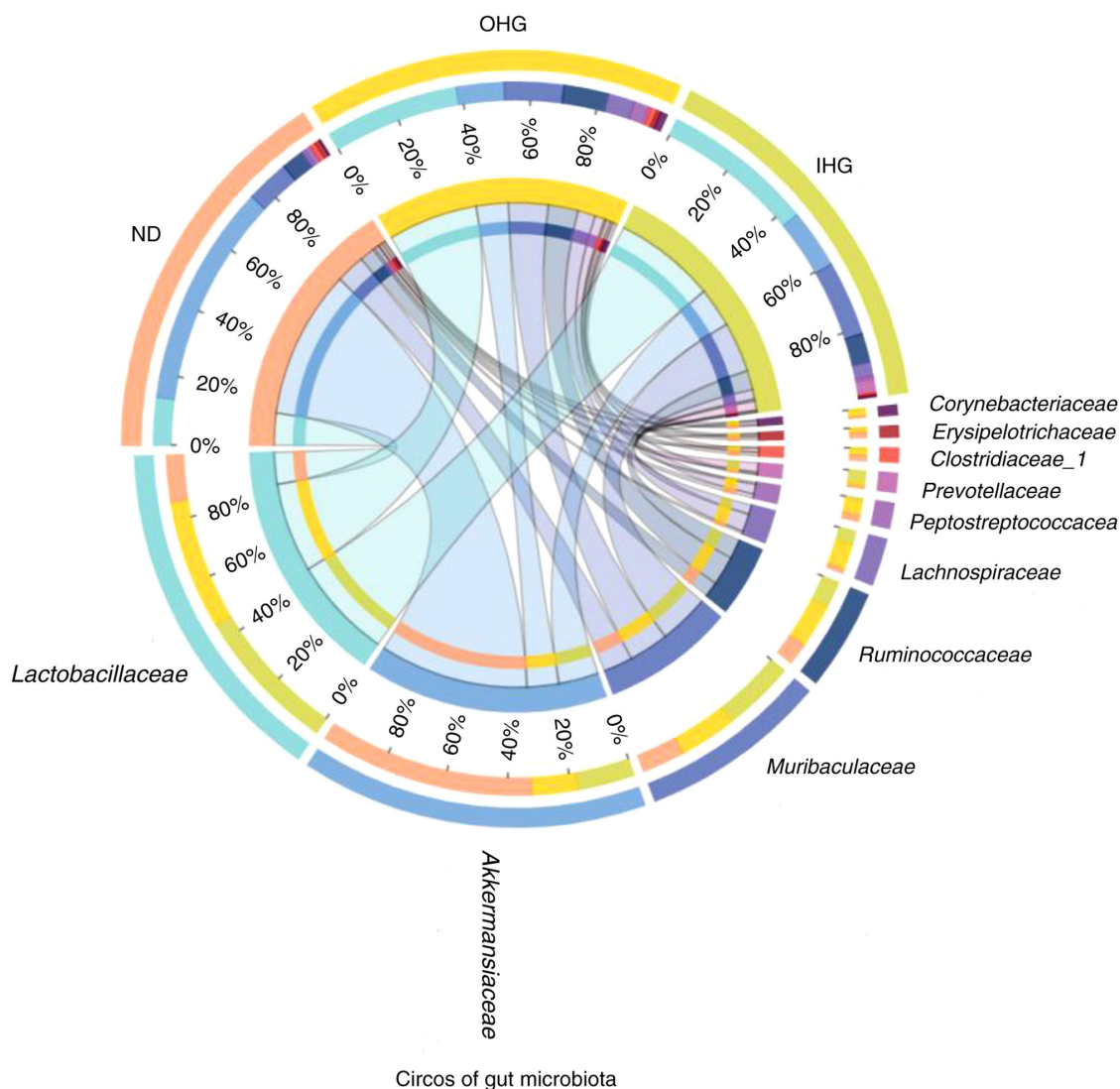


Figure 10. Circos plot of gut microbiota. Gut microbiota was altered after high glucose intake.

the early stages of the disease remains to be elucidated (27). The present study indicated that both OHG and IHG induced obvious steatosis in the livers of rats in just 2 weeks. However, there were no obvious lesions in the kidney and pancreas. The liver may be the first organ to be damaged by high glucose. Further study is required to determine whether the liver is the trigger of diabetes.

The intestinal epithelium is characterized by a remarkable self-renewal ability. The crypt base columnar cells marked by *Lgr5* represent the actively proliferating stem cells that mediate the daily renewal of the intestinal epithelium. The constant renewal cycle takes place in a hostile environment characterized by the presence of bacterial toxins and metabolites, dietary antigens and mutagens, as well as immunological cytokines and oxidative stress. The intestine has been implicated as a key organ that critically contributes to the development of obesity-associated chronic inflammation and systemic insulin resistance, as well as metabolic dysregulation (28,29). Glucose directly stimulates intestinal epithelial cells (27). The results of the present study indicated that both OHG and IHG led to jejunum mucosal injury. The damage from OHG was more serious than that of IHG. It influenced the villi and mucosa

at the same time, which may have been the result of direct contact between mucosa and high glucose.

The gastrointestinal (GI) tract is a highly complex organ composed of the intestinal epithelium layer, intestinal microbiota and local immune system. The gut microbiota is one of the most diverse communities. It constantly interacts with the cells and systems of the body. Distinct proportions of the intestinal microbiota are contained in different sections of the GI tract (30-32). Gut microbiota and its metabolites play pivotal roles in host physiology and pathology. Diet is one of the various factors influencing the microbiota. Intestinal microbiota modulate metabolism and are closely associated with epithelial cells in the intestine (33,34). The intestinal microbiota converts ingested nutrients into metabolites that target either the intestinal microbiota population or host cells. As metabolites of intestinal microbiota, SCFAs are a major energy source for intestinal epithelial cells in the colon and reinforce the intestinal barrier function through multiple mechanisms. SCFAs can reduce inflammation and protect the kidneys (35). However, lipopolysaccharides (LPS) are mainly derived from microbiota and induce inflammation and injury in the kidneys, heart, cerebrovascular as well as other organs (28).

A vast number of studies have demonstrated that the gut microbiota and their metabolites play an important role in the pathogenesis of T2DM. Accumulating evidence suggests that SCFAs regulate inflammation, energy metabolism and blood pressure, which affects kidney function through the gut-kidney axis (36,37). The present study indicated that rats treated with high glucose lost gut microbial diversity in 2 weeks. Gut microbiota was characterized by a decreased proportion of *Akkermansiaceae* and a markedly increased proportion of *Lactobacillaceae*, *Muribaculaceae*, *Ruminococcaceae* and *Peptostreptococcaceae*. As compared with the ND group, the abundance of *Akkermansiaceae* decreased in the OHG group, and the abundance of *Lactobacillaceae*, *Muribaculaceae*, *Ruminococcaceae* and *Clostridiaceae_1* increased. The abundance of *Akkermansiaceae* and *Clostridiaceae_1* decreased, while the abundance of *Lactobacillaceae* and *Muribaculaceae* increased in the IHG group. A decrease in *Akkermansiaceae* was revealed to be closely associated with obesity and diabetes (38).

Diabetic nephropathy (DN) is the leading cause of end-stage renal disease worldwide. Chronic hyperglycemia is the main risk factor for the development of DN (39,40). However, the time of DN onset remains unclear and clinical studies have yet to provide a conclusive answer. In the present study, no obvious pathological lesions were identified in the kidney tissues of the rats. However, glomerular cell swelling and mitochondria disintegration were identified, using transmission electron microscopy, after 2 weeks of high glucose intake. Apoptosis of glomerular cells was increased to a certain degree in the present study. This suggests that formation of glycotoxins in renal cells occurred quickly, however, further research is required to confirm this.

Low-grade inflammation affects the pathogenesis of the metabolic syndrome and T2DM. Chronic inflammation is considered to be one of the key factors of atherosclerosis development and is present from the earliest stages of pathology initiation. Hyperglycemia increases the magnitude and duration of systemic inflammatory responses, which promotes the development of T2DM and cardiovascular disease (41). Inflammation leads to cell apoptosis and oxidative DNA damage of the heart, liver and kidneys (42). Inflammation in the progression of steatohepatitis is a complex response to microbial dysbiosis, loss of barrier integrity in the intestine, hepatocellular stress and death, as well as inter-organ crosstalk. In response to chronic, heavy alcohol exposure, hepatocytes express a large number of chemokines and inflammatory mediators and can also release damage-associated molecular patterns during injury and death (43). Disruption of the intestinal epithelial barrier and gut vascular barrier are early events in the development of NASH (44). The present results indicated that short-term high glucose increased the systemic inflammatory responses of rats. The association between organ damage and preinflammation warrants further research.

There were some limitations in the present study. First, the dose-dependent effect of high glucose was not evaluated. Second, insulin sensitivity was not assessed. In addition, the reason why high blood glucose induced weight loss warrants further research.

In conclusion, in the present study it was revealed that high glucose may induce lesions in the liver and intestinal epithelium, disturb the balance of the gut microbiota and consequently induce inflammation. Glomerular cells were revealed to be damaged, however, no obvious pathological lesions were identified in the kidney tissues of the rats.

Acknowledgements

Not applicable.

Funding

The present study was supported by grants from the Department of Science and Technology of Guangdong Province (grant no. 2021A1515220050) and the Guangdong Provincial Bureau of Traditional Chinese Medicine (grant no. 20223001).

Availability of data and materials

The datasets used in the present study are available from the corresponding author upon reasonable request. The raw reads were deposited into the NCBI Sequence Read Archive database (accession no. PRJNA884142; ID:884142).

Authors' contributions

CM conceived and designed the study. TF, YD and WT collected and analyzed the data. XH and TW wrote the manuscript. CM, TF, WT, TW, YD and XH revised the manuscript critically for important intellectual content. CM and TF confirm the authenticity of all the raw data. All authors read and approved the final manuscript.

Ethics approval and consent to participate

All animal experiments were conducted in accordance with the committee guidelines of Guangdong Provincial People's Hospital (Guangzhou, China) and approved (approval no. KY-D-2019-082-01) by the Institutional Animal Care and Use Committee of Guangdong Provincial People's Hospital.

Patient consent for publication

Not applicable.

Competing interests

The authors declare that they have no competing interests.

References

- Dall TM, Yang W, Gillespie K, Mocarski M, Byrne E, Cintina I, Beronja K, Semilla AP, Iacobucci W and Hogan PF: The economic burden of elevated blood glucose levels in 2017: Diagnosed and undiagnosed diabetes, gestational diabetes mellitus, and prediabetes. *Diabetes Care* 42: 1661-1668, 2019.
- Cowie CC: Diabetes diagnosis and control: Missed opportunities to improve health: The 2018 Kelly West award lecture. *Diabetes Care* 42: 994-1004, 2019.
- Filla LA, Edwards JL: Metabolomics in diabetic complications. *Mol Biosyst* 12: 1090-1105, 2016.
- Zou X, Zhou X, Ji L, Yang W, Lu J, Weng J, Jia W, Shan Z, Liu J, Tian H, *et al*: The characteristics of newly diagnosed adult early-onset diabetes: A population-based cross-sectional study. *Sci Rep* 7: 46534, 2017.
- Riddle MC and Gerstein HC: The cardiovascular legacy of good glycemic control: Clues about mediators from the DCCT/EDIC study. *Diabetes Care* 42: 1159-1161, 2019.
- Gaballa M and Farag MK: Predictors of diabetic nephropathy. *Eur J Med* 8: 287-296, 2013.

7. MacIsaac RJ and Ekinci EI: Progression of diabetic kidney disease in the absence of albuminuria. *Diabetes Care* 42: 1842-1844, 2019.
8. Rines AK, Sharabi K, Tavares CD and Puigserver P: Targeting hepatic glucose metabolism in the treatment of type 2 diabetes. *Nat Rev Drug Discov* 15: 786-804, 2016.
9. Kahl S, Gancheva S, Straßburger K, Herder C, Machann J, Katsuyama H, Kabisch S, Henkel E, Kopf S, Lagerpusch M, *et al*: Empagliflozin effectively lowers liver fat content in well-controlled type 2 diabetes: A randomized, double-blind, phase 4, placebo-controlled trial. *Diabetes Care* 43: 298-305, 2020.
10. Chen M, Zheng H, Xu M, Zhao L, Zhang Q, Song J, Zhao Z, Lu S, Weng Q, Wu X, *et al*: Changes in hepatic metabolic profile during the evolution of STZ-induced diabetic rats via an ¹H NMR-based metabolomic investigation. *Biosci Rep* 39: BSR20181379, 2019.
11. Rai RC, Bagul PK and Banerjee SK: NLRP3 inflammasome drives inflammation in high fructose fed diabetic rat liver: Effect of resveratrol and metformin. *Life Sci* 253: 117727, 2020.
12. Ju M, Liu Y, Li M, Cheng M, Zhang Y, Deng G, Kang X and Liu H: Baicalin improves intestinal microecology and abnormal metabolism induced by high-fat diet. *Eur J Pharmacol* 857: 172457, 2019.
13. Zhang Y, Gu Y, Ren H, Wang S, Zhong H, Zhao X, Ma J, Gu X, Xue Y, Huang S, *et al*: Gut microbiome-related effects of berberine and probiotics on type 2 diabetes (the PREMOTEST study). *Nat Commun* 11: 5015, 2020.
14. Malik VS, Willett WC and Hu FB: Global obesity: Trends, risk factors and policy implications. *Nat Rev Endocrinol* 9: 13-27, 2013.
15. Shannon C, Merovci A, Xiong J, Tripathy D, Lorenzo F, McClain D, Abdul-Ghani M, Norton L and DeFronzo RA: Effect of chronic hyperglycemia on glucose metabolism in subjects with normal glucose tolerance. *Diabetes* 67: 2507-2517, 2018.
16. Tsuchiya K: Inflammasome-associated cell death: Pyroptosis, apoptosis, and physiological implications. *Microbiol Immunol* 64: 252-269, 2020.
17. Chiu THT, Pan WH, Lin MN and Lin CL: Vegetarian diet, change in dietary patterns, and diabetes risk: A prospective study. *Nutr Diabetes* 8: 12, 2018.
18. Taylor R and Barnes AC: Translating aetiological insight into sustainable management of type 2 diabetes. *Diabetologia* 61: 273-283, 2018.
19. Prasad M, Chen EW, Toh SA and Gascoigne NRJ: Autoimmune responses and inflammation in type 2 diabetes. *J Leukoc Biol* 107: 739-748, 2020.
20. Purnamasari D, Khumaedi AI, Soeroso Y and Marhamah S: The influence of diabetes and/or periodontitis on inflammation and adiponectin level. *Diabetes Metab Syndr* 13: 2176-2182, 2019.
21. Biscetti F, Ferraro PM, Hiatt WR, Angelini F, Nardella E, Cecchini AL, Santoliquido A, Pitocco D, Landolfi R and Flex A: Inflammatory cytokines associated with failure of lower-extremity endovascular revascularization (LER): A prospective study of a population with diabetes. *Diabetes Care* 42: 1939-1945, 2019.
22. Kheiripour N, Karimi J, Khodadadi I, Tavilani H, Goodarzi MT and Hashemnia M: Silymarin prevents lipid accumulation in the liver of rats with type 2 diabetes via sirtuin1 and SREBP-1c. *J Basic Clin Physiol Pharmacol* 29: 301-308, 2018.
23. Taylor R, Al-Mrabeh A and Sattar N: Understanding the mechanisms of reversal of type 2 diabetes. *Lancet Diabetes Endocrinol* 7: 726-736, 2019.
24. Ma Z, Fang L, Ungerfeld E, Li X, Zhou C, Tan Z, Jiang L and Han X: Supplementation of rumen-protected glucose increased the risk of disturbance of hepatic metabolism in early postpartum holstein cows. *Antioxidants (Basel)* 11: 469, 2022.
25. Bril F, Portillo Sanchez P, Lomonaco R, Orsak B, Hecht J, Tio F and Cusi K: Liver safety of statins in prediabetes or T2DM and nonalcoholic steatohepatitis: Post Hoc analysis of a randomized trial. *J Clin Endocrinol Metab* 102: 2950-2961, 2017.
26. Tsujita M, Hossain MA, Lu R, Tsuboi T, Okumura-Noji K and Yokoyama S: Exposure to high glucose concentration decreases cell surface ABCA1 and HDL biogenesis in hepatocytes. *J Atheroscler Thromb* 24: 1132-1149, 2017.
27. Leviatan S and Segal E: Identifying gut microbes that affect human health. *Nature* 587: 373-374, 2020.
28. Haase S, Haghikia A, Wilck N, Müller DN and Linker RA: Impacts of microbiome metabolites on immune regulation and autoimmunity. *Immunology* 154: 230-238, 2018.
29. Botchlett R, Li H, Guo X, Qi T, Zhao J, Zheng J, Woo SL, Pei Y, Liu M, Hu X, *et al*: Glucose and palmitate differentially regulate PFKFB3/iPKF2 and inflammatory responses in mouse intestinal epithelial cells. *Sci Rep* 6: 28963, 2016.
30. Sittipo P, Shim JW and Lee YK: Microbial metabolites determine host health and the status of some diseases. *Int J Mol Sci* 20: 5296, 2019.
31. Do MH, Lee E, Oh MJ, Kim Y and Park HY: High-glucose or -fructose diet cause changes of the gut microbiota and metabolic disorders in mice without body weight change. *Nutrients* 10: 761, 2018.
32. Zhou T, Heianza Y, Chen Y, Li X, Sun D, DiDonato JA, Pei X, LeBoff MS, Bray GA, Sacks FM and Qi L: Circulating gut microbiota metabolite trimethylamine N-oxide (TMAO) and changes in bone density in response to weight loss diets: The POUNDS lost trial. *Diabetes Care* 42: 1365-1371, 2019.
33. Lee SA, Cozzi M, Bush EL and Rabb H: Distant organ dysfunction in acute kidney injury: A review. *Am J Kidney Dis* 72: 846-856, 2018.
34. Li YJ, Chen X, Kwan TK, Loh YW, Singer J, Liu Y, Ma J, Tan J, Macia L, Mackay CR, *et al*: Dietary fiber protects against diabetic nephropathy through short-chain fatty acid-mediated activation of G protein-coupled receptors GPR43 and GPR109A. *J Am Soc Nephrol* 31: 1267-1281, 2020.
35. Liu X, Lu J, Liao Y, Liu S, Chen Y, He R, Men L, Lu C, Chen Z, Li S, *et al*: Dihydroartemisinin attenuates lipopolysaccharide-induced acute kidney injury by inhibiting inflammation and oxidative stress. *Biomed Pharmacother* 117: 109070, 2019.
36. Whitt J, Woo V, Lee P, Moncivaiz J, Haberman Y, Denson L, Tso P and Alenghat T: Disruption of epithelial HDAC3 in intestine prevents diet-induced obesity in mice. *Gastroenterology* 155: 501-513, 2018.
37. Li L, Ma L and Fu P: Gut microbiota-derived short-chain fatty acids and kidney diseases. *Drug Des Devel Ther* 11: 3531-3542, 2017.
38. Cao H, Li C, Lei L, Wang X, Liu S, Liu Q, Huan Y, Sun S and Shen Z: Stachyose improves the effects of berberine on glucose metabolism by regulating intestinal microbiota and short-chain fatty acids in spontaneous type 2 diabetic KKAY mice. *Front Pharmacol* 11: 578943, 2020.
39. Samsu N: Diabetic nephropathy: Challenges in pathogenesis, diagnosis, and treatment. *Biomed Res Int* 2021: 1497449, 2021.
40. Oshima M, Shimizu M, Yamanouchi M, Toyama T, Hara A, Furuichi K and Wada T: Trajectories of kidney function in diabetes: A clinicopathological update. *Nat Rev Nephrol* 17: 740-750, 2021.
41. Poznyak A, Grechko AV, Poggio P, Myasoedova VA, Alfieri V and Örekhov AN: The diabetes mellitus-atherosclerosis connection: The role of lipid and glucose metabolism and chronic inflammation. *Int J Mol Sci* 21: 1835, 2020.
42. Neves-Costa A and Moita LF: Modulation of inflammation and disease tolerance by DNA damage response pathways. *FEBS J* 284: 680-698, 2017.
43. Gao B, Ahmad MF, Nagy LE and Tsukamoto H: Inflammatory pathways in alcoholic steatohepatitis. *J Hepatol* 70: 249-259, 2019.
44. Mouries J, Brescia P, Silvestri A, Spadoni I, Sorribas M, Wiest R, Mileti E, Galbiati M, Invernizzi P, Adorini L, *et al*: Microbiota-driven gut vascular barrier disruption is a prerequisite for non-alcoholic steatohepatitis development. *J Hepatol* 71: 1216-1228, 2019.



This work is licensed under a Creative Commons Attribution-NonCommercial-NoDerivatives 4.0 International (CC BY-NC-ND 4.0) License.